

Study of Magnetic Field Shielding Roof of Cabin Electricity Authority Resulting in Operators Working

P. PAO-LA-OR

Power System Research Unit, School of Electrical Engineering
Institute of Engineering, Suranaree University of Technology
111 University Avenue, Muang District, Nakhon Ratchasima, 30000
THAILAND
padej@sut.ac.th

Abstract: - Monitoring, maintenance and repairing works of electric power transmission systems are main functions of power engineers in their daily schedule. Provincial Electric Authority of Thailand (PEA), state own organization in which regional power transmission systems and rural electric power distribution systems are its major services. For economic purposes, two or more circuits are normally hung on the same towers. Typically, a circuit of higher voltage is on the top of the tower. A practice of this configuration is a combination of a 115-kV power transmission line and a 22-kV distribution feeder. Safety of operators working in this circumstance depends on carefulness of all possible risks. Even when one circuit is disconnected from the supply source, magnetic induction becomes a serious issue where two or more circuits are located close enough to each other. This paper proposes a set of mathematical model of magnetic fields caused by high voltage conductors of electric power transmission systems by using a set of second-order partial differential equations. Computer-based simulation utilizing the three-dimensional finite element method (3D-FEM) is exploited as a tool for visualizing magnetic fields distribution around a power transmission line. In addition, magnetic shielding devices are investigated in order to reduce the magnetic induction on the nearby circuit. The configurations of a crane's cabin roof is studied and reported. Moreover, comparison of magnetic field distributions with and without the shielding roof is illustrated.

Key-Words: - Shielding, Cabin Roof, Transmission Line, Magnetic Fields, 3-D Finite Element Method

1 Introduction

A shield is defined as that which guards or protects. The purpose of a magnetic shield is to selectively guard against magnetic fluxes in areas of magnetic sensitivity. Shielding mechanisms can be categorized into two forms which are flux shunting and induced current shielding [1]. Two separate physical mechanisms can contribute to quasi-static materials-based magnetic shielding. In flux shunting shielding mechanism, it is based on high permeability ferromagnetic materials to attract and to divert the flux away from a shielded region. This mechanism is effective even for dc fields. The second approach, induced current shielding mechanism, is based on electrically conducting materials carrying induced currents in the presence of time-varying magnetic fields. These induced currents tend to buck out the imposed fields, again diverting the flux away from a shielded region. This mechanism is effective only for ac fields. In this research, the second approach of induced current shielding is selected for implementation. The cabin's roof material must be made from a material of high electrical conductivity, σ . When the material experiences a time-varying magnetic flux density \mathbf{B} ,

an electric field \mathbf{E} is induced within the material, as described by Faraday's Law, $\nabla \times \mathbf{E} = -(\partial \mathbf{B} / \partial t)$. If the material has some electrical conductivity, the induced electric field drives an induced current density within the material. This induced current density serves as a source for an induced magnetic flux that opposes the change in the imposed magnetic flux. The superposition of imposed and induced magnetic flux is a total flux which is bucked out of the conducting material and the shielded region on the opposite side of the material from the source.

Finite Element Method (FEM) is one of the most popular numerical methods used for computer simulation. The key advantage of the FEM over other numerical methods in engineering applications is the ability to handle nonlinear, time-dependent and circular geometry problems. Therefore, this method is suitable for solving the problem involving magnetic field effects around the transmission line caused by circular cross-section of high voltage conductors. Especially, when safety of field operators is the highest priority under consideration, the region domain must be carefully determined. Although the conventional methods are simpler than

the use of the FEM, they are limited for the system of simple geometry. In practice, several metallic structures can be found underneath the power transmission line, e.g. steel tower trusts, communication lines nearby, metallic fends or other lower voltage transmission lines. Employing the FEM can include these effects by choosing material for each additional structure domain. With this feature, the FEM is one of potential numerical simulation tools for analyzing magnetic field problems of combined material regions. In [2-4], FEM is used to study the effect of various shield geometries and shield materials around a high current carrying cables used in power transmission lines. Two-dimensional analysis is sufficient for this problem because the cables are very long compared to the wire diameters. In [5], presented a theoretical analysis of a two-dimensional model of power-frequency magnetic field shielding with flat sheets in a source of long conductors. Shielding principles taking into account geometric and material parameters are presented based on the simplification of closed-form expressions. The installation of auxiliary loop conductors near phase conductors of overhead power lines has been proposed [6-8]. In some cases, a series capacitor is inserted to obtain a sufficient auxiliary loop current [7]. From literature, magnetic field shielding of power transmission lines is focused on blocking interference from sources of fields along the transmission lines. No report describes work concerning the shielding at the point of operation. This research contributes the attention to build some equipment attached with or close to operators to reject or neutralize any magnetic fields that might cause some severe problems. This equipment is based on the induced current shielding mechanism. It is designed as a roof to cover field operators and therefore is expected to isolate operators from any magnetic field induction around or onto them. A 115-kV power transmission line of Provincial Electricity Authority (PEA) in Nakhon Ratchasima province of Thailand hung over a 22-kV power distribution line on the same tower is selected for test. Computer-based simulation utilizing the three-dimensional finite element method (3D-FEM) in the time harmonic mode, instructed in MATLAB programming environment with graphical representation for magnetic field strength have been evaluated.

In this paper, magnetic field modelling of power transmission lines is briefed in Section 2. Section 3 is to illustrate the utilization of the 3D-FEM by using Galerkin approach for the magnetic field modelling described in Section 2. The domain of study with the 3D-FEM can be discretized by using

linear tetrahedron elements. Section 4 gives simulation results of no shielding roof installed. Test cases given in this paper is the 115-kV power transmission line hung over a 22-kV power distribution line on the same tower. It is assumed that field operators can access directly to touch power lines by crane's cabin support. The simulation conducted herein is based on the 3D-FEM method given in Section 3. All the programming instructions are coded in MATLAB program environment. Section 5 gives simulation results of the presence of the shielding roof. The last section gives conclusion and future work.

2 Modeling of Magnetic Fields for a Power Transmission Line

The mathematical model representing magnetic fields (\mathbf{B}) caused by a power transmission line carrying high current is expressed in form of the magnetic field intensity (\mathbf{H}) in which $\mathbf{B} = \mu\mathbf{H}$. Utilizing the wave equation (Helmholtz's equation) as in (1) [9-10], magnetic field modeling that follows the Ampere's circuital law is defined.

$$\nabla^2 \mathbf{H} - \sigma\mu \frac{\partial \mathbf{H}}{\partial t} - \varepsilon\mu \frac{\partial^2 \mathbf{H}}{\partial t^2} = 0 \quad (1)$$

where ε is the constant dielectric permittivity, μ is the magnetic permeability, and σ is the electrical conductivity.

This paper has considered the time-harmonic system by representing $\mathbf{H} = H e^{j\omega t}$ [11], therefore

$$\frac{\partial \mathbf{H}}{\partial t} = j\omega H \quad \text{and} \quad \frac{\partial^2 \mathbf{H}}{\partial t^2} = -\omega^2 H$$

where ω is the angular frequency.

Therefore, refer to (1) can be rewritten into the following equation.

$$\nabla^2 H - j\omega\sigma\mu H + \omega^2\varepsilon\mu H = 0$$

Considering the problem in three-dimensional (x, y, z) plane, then

$$\frac{\partial}{\partial x} \left(\frac{1}{\mu} \frac{\partial H}{\partial x} \right) + \frac{\partial}{\partial y} \left(\frac{1}{\mu} \frac{\partial H}{\partial y} \right) + \frac{\partial}{\partial z} \left(\frac{1}{\mu} \frac{\partial H}{\partial z} \right) - (j\omega\sigma - \omega^2\varepsilon)H = 0 \quad (2)$$

As can be seen, to obtain an exact solution of (2) is difficult. In this paper, the FEM has been employed to find an approximate solution [12-15].

3 3D-FEM for power transmission lines

3.1 Discretization

This paper conducts the simulation study by considering the 115-kV PEA's transmission system in Nakhon Ratchasima province. This type of power transmission systems is common in rural areas in Thailand. The selected test system consists of 2-bundle conductors configuring in vertical conductor arrangement as shown in Fig. 1. Also, a 22-kV power line in horizontal conductor arrangement is hung below the HV transmission line. Fig. 2 depicts the detail of the power lines.

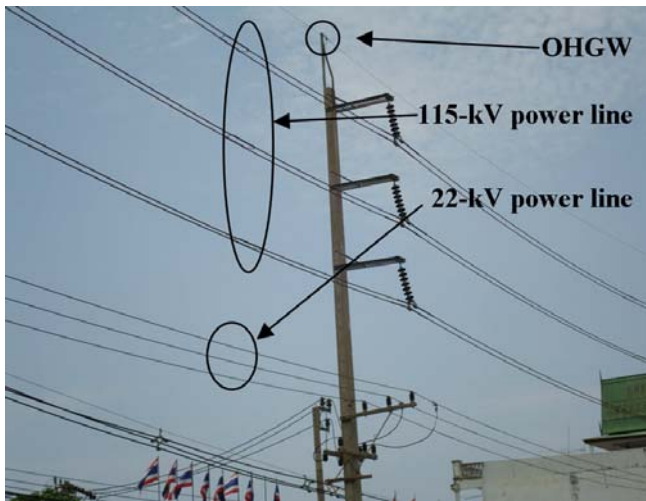


Fig.1 Power lines in Nakhon Ratchasima province

In this work, maintenance of electric power transmission lines is carried out by field operators which are lifted over the ground by a crane's cabin support system. In practice, it is typical to see two or more power line circuits hung at the same tower. If one circuit needs maintenance, the source of that circuit is then disconnected. In addition, two end of the opened line is normally grounded. Unfortunately, if there exists one or more circuits carrying load current on the same tower, induced voltage on the maintenance circuit is distributed from one end to another end uniformly. Although at the two ends of the line the value of the induced voltage is grounded, induced voltage over kilo-volt (kV) is possible somewhere between the two ends. This can cause some serious injury to the maintenance operators. In this paper, a 1-m³ of crane's cabin covered with insulation is modelled.

Under operation, it is lifted about 12 m above the ground. It is assumed that there exist two power circuits on the same tower. One circuit is a 115-kV power transmission line on the top and another is a 22-kV power distribution feeder hung underneath. An operator working on the cabin is represented by a box of 1.8×0.2×0.5 m³ located at the center of the cabin. The cabin is just 0.5-m away from the 22-kV power distribution circuit. This can be illustrated in Fig. 3. The region of study is a larger domain of 15 × 20 × 30 m³. As shown in Fig. 4, this box can capture line portion of the two circuits with 20-m in length. The domain of study with the 3D-FEM can be discretized by using linear tetrahedron elements. This can be accomplished by using Gmsh [16] for 3D grid generation. Fig. 5 displays grid representation of the test system. The region domain consists of 33576 nodes and 214503 elements. Fig. 6 shows the surface grid of the entire domain for viewing purpose.

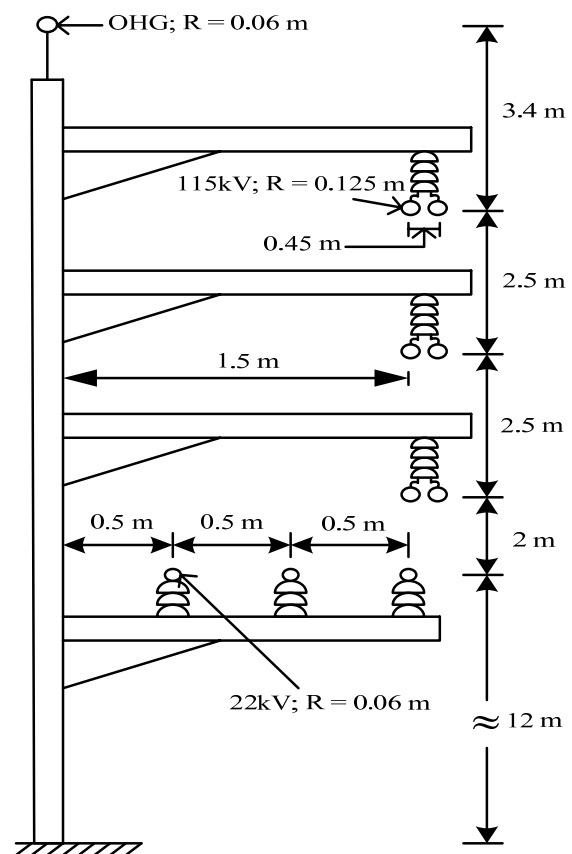


Fig.2 Detail of the power lines

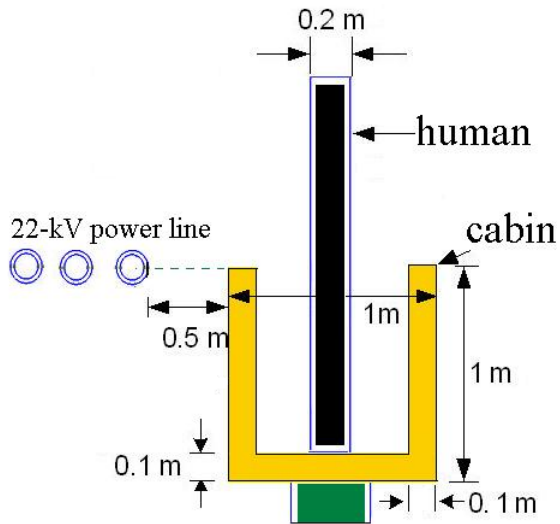


Fig.3 Modeling of crane's cabin with an operator

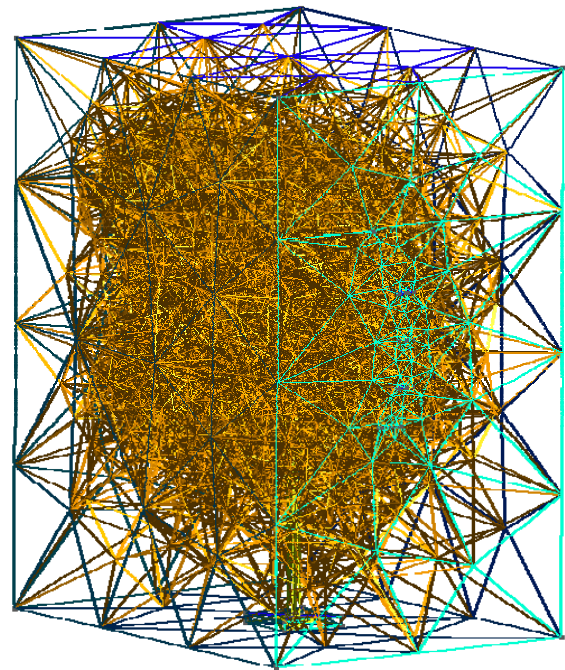


Fig. 5 Discretization of the entire domain given in Fig. 4

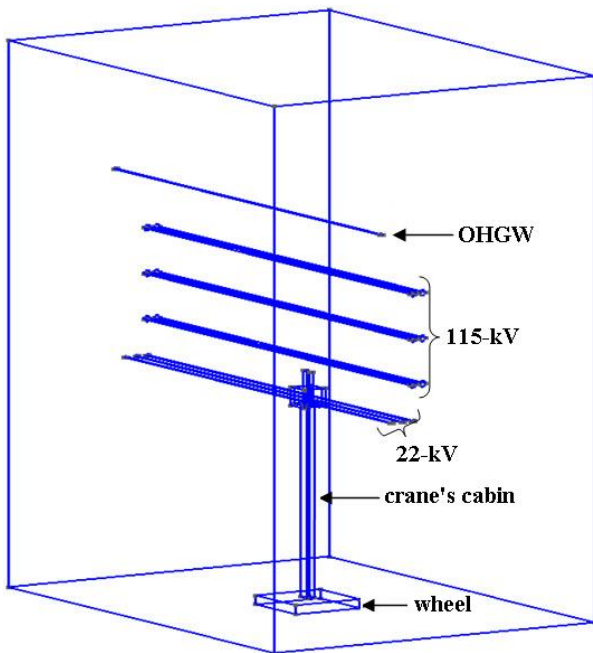


Fig. 4 Entire domain of study

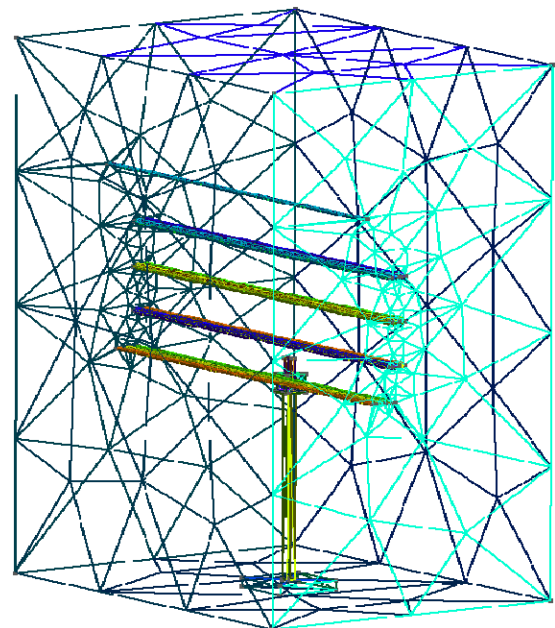


Fig. 6 Surface grid of the entire domain

3.2 3D-FEM Formulation

An equation governing each element is derived from the Maxwell's equations directly by using Galerkin approach, which is the particular weighted residual method for which the weighting functions are the same as the shape function. The shape function for 3D-FEM used in this research is the application of

4-node tetrahedron element (three-dimensional linear element) [17-19]. According to the method, the magnetic field intensity is expressed as follows

$$H(x, y, z) = H_1N_1 + H_2N_2 + H_3N_3 + H_4N_4 \quad (3)$$

where N_i , $i = 1, 2, 3, 4$ is the element shape function and the H_i , $i = 1, 2, 3, 4$ is the approximation of the magnetic field intensity at each node (1, 2, 3, 4) of the elements, which is

$$N_i = \frac{1}{6V}(a_i + b_i x + c_i y + d_i z)$$

where V is the volume of the tetrahedron element, which is expressed as

$$V = \frac{1}{6} \begin{vmatrix} 1 & x_1 & y_1 & z_1 \\ 1 & x_2 & y_2 & z_2 \\ 1 & x_3 & y_3 & z_3 \\ 1 & x_4 & y_4 & z_4 \end{vmatrix}$$

and

$$\begin{aligned} a_1 &= x_4(y_2z_3 - y_3z_2) + x_3(y_4z_2 - y_2z_4) + x_2(y_3z_4 - y_4z_3) \\ a_2 &= x_4(y_3z_1 - y_1z_3) + x_3(y_1z_4 - y_4z_1) + x_1(y_4z_3 - y_3z_4) \\ a_3 &= x_4(y_1z_2 - y_2z_1) + x_2(y_4z_1 - y_1z_4) + x_1(y_2z_4 - y_4z_2) \\ a_4 &= x_3(y_2z_1 - y_1z_2) + x_2(y_1z_3 - y_3z_1) + x_1(y_3z_2 - y_2z_3) \end{aligned}$$

$$\begin{aligned} b_1 &= y_4(z_3 - z_2) + y_3(z_2 - z_4) + y_2(z_4 - z_3) \\ b_2 &= y_4(z_1 - z_3) + y_1(z_3 - z_4) + y_3(z_4 - z_1) \\ b_3 &= y_4(z_2 - z_1) + y_2(z_1 - z_4) + y_1(z_4 - z_2) \\ b_4 &= y_3(z_1 - z_2) + y_1(z_2 - z_3) + y_2(z_3 - z_1) \end{aligned}$$

$$\begin{aligned} c_1 &= x_4(z_2 - z_3) + x_2(z_3 - z_4) + x_3(z_4 - z_2) \\ c_2 &= x_4(z_3 - z_1) + x_3(z_1 - z_4) + x_1(z_4 - z_3) \\ c_3 &= x_4(z_1 - z_2) + x_1(z_2 - z_4) + x_2(z_4 - z_1) \\ c_4 &= x_3(z_2 - z_1) + x_2(z_1 - z_3) + x_1(z_3 - z_2) \end{aligned}$$

$$\begin{aligned} d_1 &= x_4(y_3 - y_2) + x_3(y_2 - y_4) + x_2(y_4 - y_3) \\ d_2 &= x_4(y_1 - y_3) + x_1(y_3 - y_4) + x_3(y_4 - y_1) \\ d_3 &= x_4(y_2 - y_1) + x_2(y_1 - y_4) + x_1(y_4 - y_2) \\ d_4 &= x_3(y_1 - y_2) + x_1(y_2 - y_3) + x_2(y_3 - y_1) \end{aligned}$$

The method of the weighted residual with Galerkin approach is then applied to the differential equation, refer to (2), where the integrations are performed over the element domain Ω .

$$\int_{\Omega} N_i \left(\frac{\partial}{\partial x} \left(\frac{1}{\mu} \frac{\partial H}{\partial x} \right) + \frac{\partial}{\partial y} \left(\frac{1}{\mu} \frac{\partial H}{\partial y} \right) + \frac{\partial}{\partial z} \left(\frac{1}{\mu} \frac{\partial H}{\partial z} \right) \right) d\Omega - \int_{\Omega} N_i (j\omega\sigma - \omega^2\varepsilon) H d\Omega = 0$$

, or in the compact matrix form

$$[M + K]\{H\} = 0 \quad (4)$$

$$\begin{aligned} M &= (j\omega\sigma - \omega^2\varepsilon) \int_{\Omega} N_i N_j d\Omega \\ &= \frac{(j\omega\sigma - \omega^2\varepsilon)V}{20} \begin{bmatrix} 2 & 1 & 1 & 1 \\ 1 & 2 & 1 & 1 \\ 1 & 1 & 2 & 1 \\ 1 & 1 & 1 & 2 \end{bmatrix} \end{aligned}$$

$$\begin{aligned} K &= \frac{1}{\mu} \int_{\Omega} \left(\frac{\partial N_i}{\partial x} \frac{\partial N_j}{\partial x} + \frac{\partial N_i}{\partial y} \frac{\partial N_j}{\partial y} + \frac{\partial N_i}{\partial z} \frac{\partial N_j}{\partial z} \right) d\Omega \\ &= \frac{1}{36\mu V} \begin{bmatrix} b_1b_1 + c_1c_1 + d_1d_1 & b_1b_2 + c_1c_2 + d_1d_2 \\ b_1b_2 + c_1c_2 + d_1d_2 & b_2b_2 + c_2c_2 + d_2d_2 \\ b_1b_3 + c_1c_3 + d_1d_3 & b_2b_3 + c_2c_3 + d_2d_3 \\ b_1b_4 + c_1c_4 + d_1d_4 & b_2b_4 + c_2c_4 + d_2d_4 \\ b_1b_3 + c_1c_3 + d_1d_3 & b_1b_4 + c_1c_4 + d_1d_4 \\ b_2b_3 + c_2c_3 + d_2d_3 & b_2b_4 + c_2c_4 + d_2d_4 \\ b_3b_3 + c_3c_3 + d_3d_3 & b_3b_4 + c_3c_4 + d_3d_4 \\ b_3b_4 + c_3c_4 + d_3d_4 & b_4b_4 + c_4c_4 + d_4d_4 \end{bmatrix} \end{aligned}$$

For one element containing 4 nodes, the expression of the FEM approximation is a 4x4 matrix. With the account of all elements in the system of n nodes, the system equation is sizable as an $n \times n$ matrix.

4 3D-FEM Simulation Result

The boundary conditions applied here are zero magnetic fields at the ground, and the OHGW and the disconnected 22-kV power lines. For the boundary conditions at outer perimeters of 115-kV power lines has applied with the research of [20-21],

which boundary conditions of magnetic field depends on the load current. In cabin and crane's cabin support which are covered by insulation, Neumann conditions ($\partial\mathbf{H}/\partial\mathbf{n} = 0$) are exploited. This simulation uses the system frequency of 50 Hz. Both power lines are bared conductors of Aluminum Conductor Steel Reinforced (ACSR). Properties of materials used for this simulation is given in Table 1 [22]. It notes that the permeability of free space (μ_0) = $4\pi \times 10^{-7}$ H/m and the permittivity of free space (ϵ_0) = 8.854×10^{-12} F/m.

Table 1 Properties of materials for simulation

| Description | Electrical Conductivity (σ , S/m) | Relative Permeability (μ_r) | Relative Permittivity (ϵ_r) |
|---------------|---|-----------------------------------|--|
| Power Lines | 0.8×10^7 | 300 | 3.5 |
| Human | 0.21 | 18.8 | 5.0 |
| Cabin | 0.1 | 8.0 | 1.17 |
| Crane's Cabin | 0.1 | 8.0 | 1.17 |
| Wheel | 0.004 | 1.089 | 7.0 |
| Air | 0 | 1.0 | 1.0 |

The FEM-based simulation conducted in this paper is coded with MATLAB programming for calculation of magnetic field dispersion. For which 3D-FEM result, that can be graphically presented in the filled polygon of magnetic fields dispersed thoroughly the volume of study. Fig.7 illustrates the result of magnetic field distribution of 3D-FEM for a test case. Fig.8 illustrates the result of magnetic field contours on the cross-sectional area perpendicular to the z axis, where the cutaway position is given at the center of the operator body. The simulation results showed that the value of magnetic field distribution close to conductor surfaces is higher than those far from the conductor surfaces. The lowest field occurred at the ground level. In addition, the average value of magnetic flux density acting on the operator can be calculated by using the software and this is as high as $22.6136 \mu\text{T}$ which can cause harm to operators.

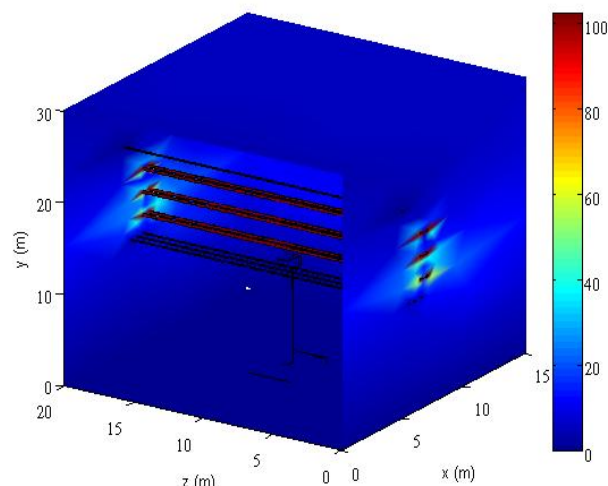


Fig.7 Magnetic field distribution (μT) of the region domain

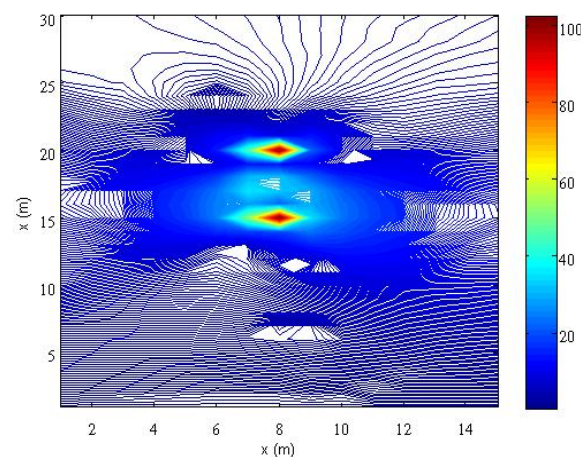


Fig.8 Magnetic field contour (μT) at a cutaway position of the center of the operator body

5 Magnetic Field Shielding with Cabin Roof

In this paper, the induced current shielding mechanism is exploited to design the roof of magnetic shielding. Aluminum has high electrical conductivity, therefore it is selected to be used as the roof material. Aluminum has some properties as i) electrical conductivity is 3.82×10^7 S/m, ii) relative permeability, μ_r , is 1.0 and iii) relative permittivity, ϵ_r , is 8.8 [23]. The roof of aluminum sheet is 8-mm in depth supported by four poles at each corner as shown in Fig. 9. The roof of aluminum sheet can be bended to adjust angle of shielding, e.g. 45° , as described in the figure.

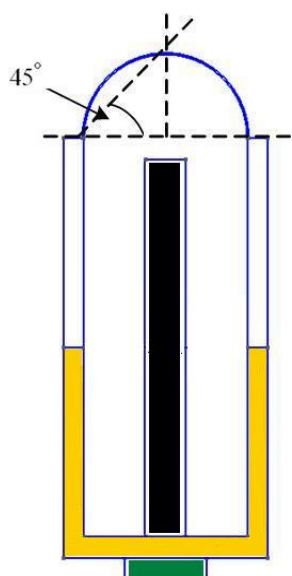
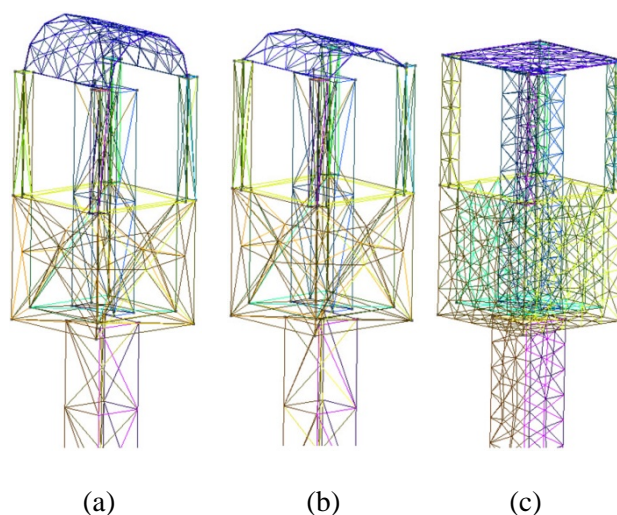
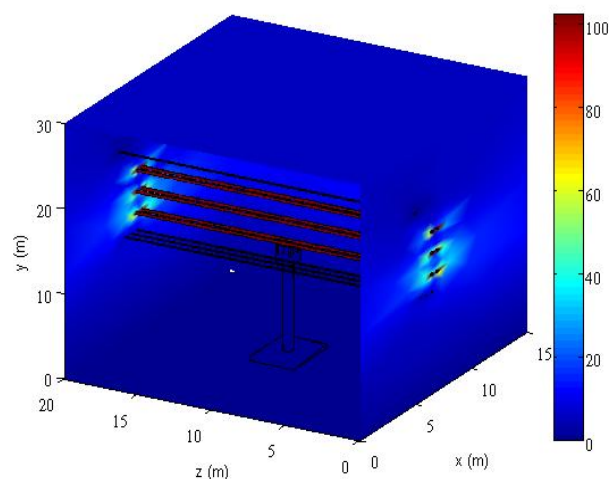
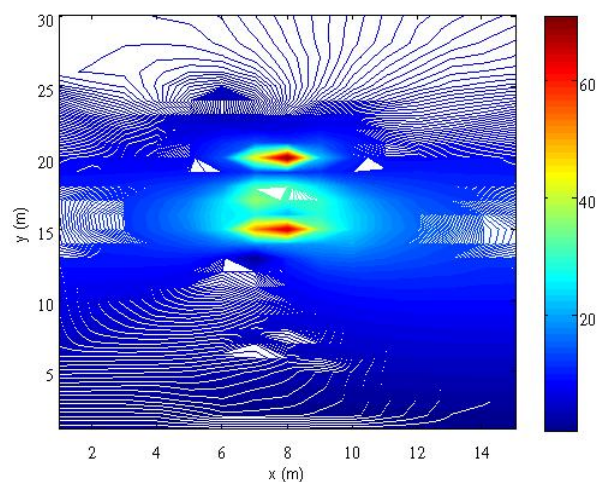


Fig.9 Modeling of cabin roof

In this paper, angle of shielding according to the aluminum sheet bending is varied as 45° , 40° , 35° , 30° , 25° , 20° , 15° , 10° , 5° and 0° . Fig. 10(a), Fig. 10(b) and Fig. 10(c) gave three-dimensional grid of the selected angles at 45° , 10° and 0° , respectively. Fig.11, Fig.13 and Fig.15 illustrated the result of magnetic field distribution of 3D-FEM for the angle cases of 45° , 10° and 0° , respectively. Fig.12, Fig.14 and Fig.16 illustrated the result of magnetic field contours on the cross-sectional area, where the cutaway position is given at the center of the operator body as the same case as in Fig. 11, 13 and 15, respectively. With the roof of shielding, the magnetic field distribution is remarkably changed. It is due to the induced current shielding mechanism created by using electrically conducting materials carrying the induced currents. These induced currents tend to buck out the imposed fields, again diverting the flux away from a shielded region. Furthermore, the average value of the magnetic flux density acting on the operator can be obtained and illustrated in Table 2.

Fig.10 3-D grid of the crane's bended cabin roof
(a) 45° , (b) 10° and (c) 0° Fig.11 Magnetic field distribution (μT) for angle case 45° Fig.12 Magnetic field contour (μT) at a cutaway position of the center of the operator body for angle case 45°

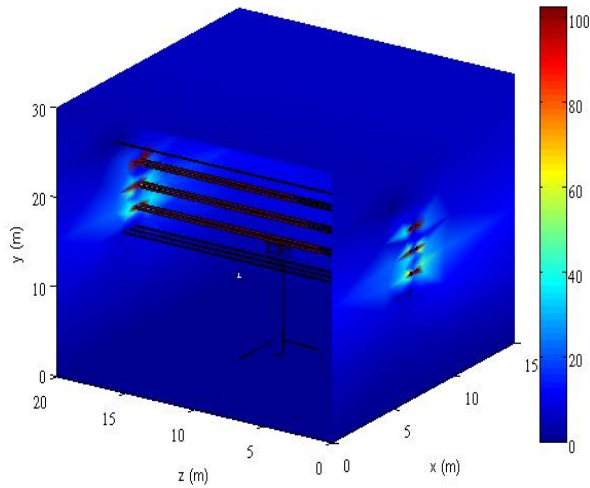


Fig.13 Magnetic field distribution (μT) for angle case 10°

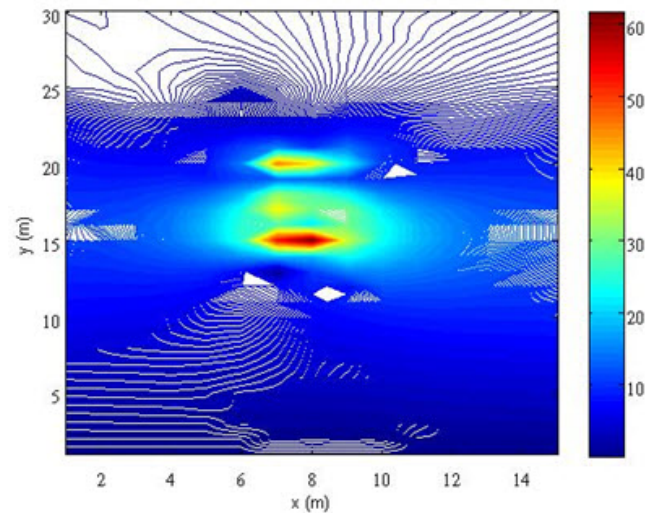


Fig.16 Magnetic field contour (μT) at a cutaway position of the center of the operator body for angle case 0°

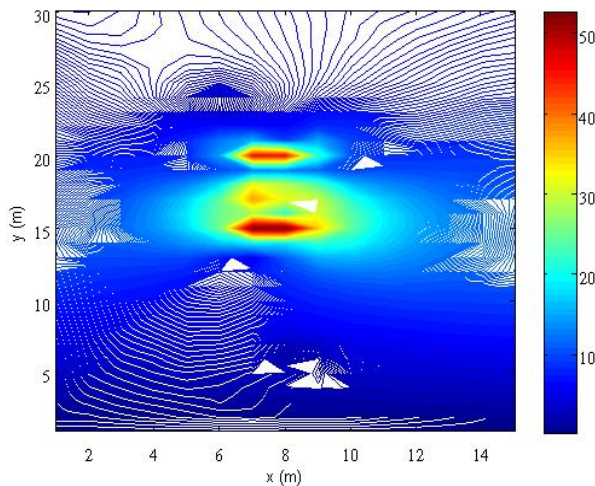


Fig.14 Magnetic field contour (μT) at a cutaway position of the center of the operator body for angle case 10°

Table 2 Average magnetic flux density acting on the operator body

| Angle | Magnetic Field (μT) | Angle | Magnetic Field (μT) |
|------------|----------------------------|------------|----------------------------|
| 0° | 10.0221 | 25° | 11.0582 |
| 5° | 10.2067 | 30° | 11.0312 |
| 10° | 9.7579 | 35° | 10.1973 |
| 15° | 11.4373 | 40° | 10.7260 |
| 20° | 11.2465 | 45° | 10.8994 |

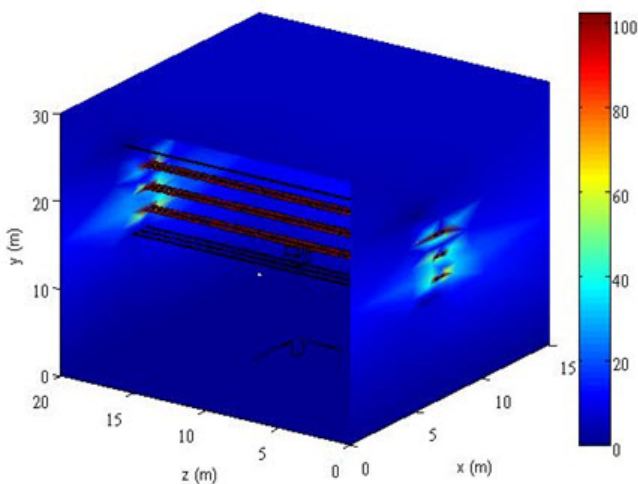


Fig.15 Magnetic field distribution (μT) for angle case 0°

From Table 2, the bended roof angle of 10° degree can considerably reduce the magnetic flux density acting on the operator with the lowest average value. In this case, the magnetic flux density is just only $9.7579 \mu T$. It is noted that $22.6136 \mu T$ is the value of the magnetic flux density without shielding equipment. Therefore, the shielding efficiency (SE) at this condition, is $SE = 20 \log (22.6136/9.7579) = 7.3 \text{ dB}$. This strongly confirms that the installation of the crane's cabin roof can efficiently suppress the magnetic fields generated from other sources nearby which might cause some injury to the operator.

6 Conclusion

This paper presents design and simulation of magnetic field shielding equipment based on the induced current shielding mechanism. Operators working at power transmission tower having two or more circuits are focused. Roof of the crane's cabin with the field operator working inside is designed. A high electrical conductivity material, aluminium, was used to be the roof material. The aluminium sheet was bended to adjust the roof angle in a range of $0^\circ - 45^\circ$ with 5° increment. A 115-kV power transmission line of Provincial Electricity Authority (PEA) in Nakhon Ratchasima province of Thailand hung over a 22-kV power distribution line on the same tower was selected for test. The computer simulation is performed by using 3D finite element method (3D-FEM) instructed in MATLAB programming codes. As a result, the roof of the 10° -bended angle gives the most reduction of the magnetic flux density acting on the field operator. At this design angle, the shielding efficiency is 7.3 dB.

References:

- [1] J.F. Hoburg, Principles of Quasistatic Magnetic Shielding with Cylindrical and Spherical Shields, *IEEE Transactions on Electromagnetic Compatibility*, Vol. 37, No. 4, 1995, pp.574-579.
- [2] K. Wassef, V.V. Varadan and V.K. Varadan, Magnetic Field Shielding Concepts for Power Transmission Lines, *IEEE Transactions on Magnetics*, Vol. 34, No. 3, 1998, pp.649-654.
- [3] L. Hasselgren and J. Luomi, Geometrical Aspects of Magnetic Shielding at Extremely Low Frequencies, *IEEE Transactions on Electromagnetic Compatibility*, Vol. 37, No. 3, 1995, pp.409-420.
- [4] M.A. Kolbehdari, Quasi-Static Characteristic of a Shielded Cylindrical Coupled Microstrip Transmission Line by Finite-Element Method, *Proceedings of Southeastcon'94 IEEE*, 1994, pp.170-174.
- [5] Y. Du, T.C. Cheng and A.S. Farag, Principles of Power-Frequency Magnetic Field Shielding with Flat Sheets in a Source of Long Conductors, *IEEE Transactions on Electromagnetic Compatibility*, Vol. 38, No. 3, 1996, pp.450-459.
- [6] K. Yamazaki, T. Kawamoto and H. Fujinami, Requirement for Power Line Magnetic Field Mitigation Using a Passive Loop Conductor, *IEEE Transactions on Power Delivery*, Vol. 15, No. 2, 2000, pp.646-651.
- [7] R.A. Walling, J.J. Paserba and C.W. Burns, Series-Capacitor Compensated Shield Scheme for Enhanced Mitigation of Transmission Line Magnetic Fields, *IEEE Transactions on Power Delivery*, Vol. 8, No. 1, 1993, pp.461-468.
- [8] A.R. Memari and W. Janischewskyj, Mitigation of Magnetic Field near Power Lines, *IEEE Transactions on Power Delivery*, Vol. 11, No. 3, 1996, pp.1577-1586.
- [9] M.V.K. Chari and S.J. Salon, *Numerical Methods in Electromagnetism*, Academic Press, USA, 2000.
- [10] M. Weiner, *Electromagnetic Analysis Using Transmission Line Variables*, World Scientific Publishing, Singapore, 2001.
- [11] C. Christopoulos, *The Transmission-Line Modeling Method: TLM*, IEEE Press, USA, 1995.
- [12] P. Pao-la-or, T. Kulworawanichpong, S. Sujitjorn and S. Peaiyoung, Distributions of Flux and Electromagnetic Force in Induction Motors: A Finite Element Approach, *WSEAS Transactions on Systems*, Vol.5, No.3, 2006, pp. 617-624.
- [13] P. Pao-la-or, S. Sujitjorn, T. Kulworawanichpong and S. Peaiyoung, Studies of Mechanical Vibrations and Current Harmonics in Induction Motors Using Finite Element Method, *WSEAS Transactions on Systems*, Vol.7, No.3, 2008, pp. 195-202.
- [14] P. Pao-la-or, A. Isaramongkolrak and T. Kulworawanichpong, Study of Influence of an Overhead Ground Wire on Electric Fields around the HV Power Transmission Line Using 2D and 3D Finite Element Method, *WSEAS Transactions on Power Systems*, Vol. 3, No. 11, 2008, pp.675-684.
- [15] P. Pao-la-or, A. Isaramongkolrak and T. Kulworawanichpong, Finite Element Analysis of Magnetic Field Distribution for 500-kV Power Transmission Systems, *Engineering Letters*, Vol. 18, No. 1, 2010, pp.1-9.
- [16] C. Geuzaine and J-F. Remacle. (2009, September 21). Gmsh: a three-dimensional finite element mesh generator with built-in pre- and post-processing facilities (Version 2.4.2) [Online]. Available: <http://geuz.org/gmsh>
- [17] R.W. Lewis, P. Nithiarasu and K.N. Seetharamu, *Fundamentals of the Finite Element Method for Heat and Fluid Flow*, John Wiley & Sons, USA, 2004.
- [18] M.A. Bhatti, *Advanced Topics in Finite Element Analysis of Structures*, John Wiley & Sons, USA, 2006.
- [19] P.I. Kattan, *MATLAB Guide to Finite Elements (2nd edition)*, Springer Berlin Heidelberg, USA, 2007.

- [20] P. Pin-anong, *The Electromagnetic Field Effects Analysis which Interfere to Environment near the Overhead Transmission Lines and Case Study of Effects Reduction*, M. Eng. Thesis, King Mongkut's Institute of Technology Ladkrabang, Bangkok, Thailand, 2002.
- [21] G.B. Iyyuni and S.A. Sebo, Study of Transmission Line Magnetic Fields, *Proceedings of the Twenty-Second Annual North American, IEEE Power Symposium*, 1990, pp.222-231.
- [22] Jr.W.H. Hayt and J.A. Buck, *Engineering Electromagnetics (7th edition)*, McGraw-Hill, Singapore, 2006.
- [23] J.C. Lopez, P.C. Romero and P. Dular, Parametric analysis of magnetic field mitigation shielding for underground power cables, *Proceedings of the International Conference on Renewable Energies and Power Quality*, 2003, pp.326-333.